

# Plaquette Order in a Frustrated Spin-Peierls Ladder

Ofer Shlagman and Efrat Shimshoni

*Department of Physics, Bar Ilan University, Ramat-Gan 52900, Israel*

We study the effect of spin-Peierls instability on the phase-diagram of a frustrated antiferromagnetic spin-1/2 ladder, with weak transverse and diagonal rung coupling. Our analysis focuses on a one-dimensional version of the model (i.e. a single two-leg ladder) where we consider two forms of spin-Peierls (SP) instabilities on the legs: columnar dimers (CD) and staggered dimers (SD). We particularly examine the regime of parameters (corresponding to an intermediate XXZ anisotropy) where the SP and rung coupling terms are equally relevant. In both the CD and SD cases we find that the effective field theory describing the system is a self-dual sine-Gordon model, which favors ordering and the opening of a gap to excitations. The order parameter, which reflects the interplay between the SP and rung interactions, represents a crystal of 4-spin plaquettes on which longitudinal and transverse dimers are in a superposition. Depending on the SP instability mode these plaquettes are closed or open, however both types spontaneously break reflection symmetry across the ladder. The closed plaquettes are stable, while the open plaquette-order is relatively fragile and the corresponding gap may be tuned to zero under extreme conditions. We further find that a first order transition occurs from the Plaquette order to a valence bond crystal (VBC) of dimers on the legs. It is suggestive that in a higher dimensional version of this system, this variety of distinct VBC states with comparable energies leads to the formation of domains. Effectively one-dimensional gapless spinon modes on domain boundaries can possibly account for the experimental observation of a spin-liquid behavior in a physical realization of the model.

## I. INTRODUCTION

Low dimensional quantum magnets attract a lot of experimental and theoretical attention, due to the rich physics arising from their enhanced quantum fluctuations, and competing interactions which often induce nonclassical ground states. Most prominently, quantum effects are manifested by spin- $\frac{1}{2}$  systems at one dimension (1D). The simplest model for 1D quantum antiferromagnets is the XXZ Hamiltonian, describing a spin- $\frac{1}{2}$  chain with nearest neighbor interactions<sup>1</sup>,

$$H = \sum_i J_{xy} (S_{i+1}^x S_i^x + S_{i+1}^y S_i^y) + J_z \sum_i S_{i+1}^z S_i^z \quad (1)$$

where  $J_\alpha > 0$  corresponds to antiferromagnetic exchange interaction. The isotropic case  $J_{xy} = J_z$  yields the 1D Heisenberg model. This system has a nonclassical ground state at  $T = 0$  known as 'spin-liquid', that is characterized by a lack of long range order and power law decay of the spin-spin correlations. The properties of the 1D spin-liquid at low temperatures can be evaluated in terms of gapless spin- $\frac{1}{2}$  excitations named spinons, which can be represented as interacting spinless Fermions and form a Luttinger liquid.

Whether the spin-liquid state can also be found in higher dimensions, and under what conditions, is an im-

portant question<sup>2</sup>. Typically, the 1D spin-liquid state is unstable to interchain couplings which tend to favor various types of long-range order<sup>3-7</sup>. Therefore, a necessary condition is the presence of frustration resulting from conflict between competing interactions. A particular interesting model for frustrated spin-systems, on a 2D cubic lattice, was introduced by Nersesyan and Tsvelik<sup>8</sup> (NT) as a possible realization of the long-sought resonating valence bond (RVB) state<sup>9</sup>. The model is described

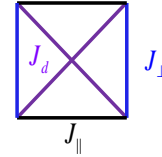


FIG. 1: (color online) schematic representation of the exchange interactions of the NT model.

by the Hamiltonian

$$H = \sum_{j,\nu} \{ J_{\parallel} \mathbf{S}_{j,\nu} \cdot \mathbf{S}_{j+1,\nu} + \sum_{\mu=\pm 1} [J_{\perp} \mathbf{S}_{j,\nu} + J_d (\mathbf{S}_{j+1,\nu} + \mathbf{S}_{j-1,\nu})] \cdot \mathbf{S}_{j,\nu+\mu} \}, \quad (2)$$

where  $\nu$  enumerates chains and  $j$  is the site number,  $J_{\parallel}$  is

the intrachain exchange constant which couples neighbor-

ing spins on the same chain, and  $J_{\perp}, J_d$  are the transverse and diagonal interchain exchange constants respectively. The interactions of this model are presented in Fig. 1. The competition between exchange interactions on each triangle prevents antiferromagnetic ordering. The model is particularly interesting for the maximally frustrated special ratio  $J_{\perp}/J_d = 2$ , which corresponds to a critical point between two phases of valence bond crystal (VBC); i.e. a state where pairs of spins form singlets (valence bonds) which are localized, thus forming an ordered crystal. In the anisotropic limit ( $J_{\parallel} \gg J_{\perp} = 2J_d$ ) of weakly coupled chains, the ground state at this critical point was first argued to be an RVB state<sup>8,10</sup>: a state where valence bonds undergo quantum fluctuations. The ground state is then a superposition of different partitionings of spins into valence bonds with no preference for any specific valence bond. However, since then it was argued that the ground state could still be a VBC<sup>11–13</sup>.

Recently, an experimental group has measured the thermodynamic properties of the material (NO)[Cu(NO<sub>3</sub>)<sub>3</sub>] (NOCuNO)<sup>14</sup>, which appears to be a good realization of the NT model in the weak coupling regime ( $J_{\perp} \ll J_{\parallel}$ ). NOCuNO has the unique feature that due to the symmetry of the crystal structure its exchange interactions obey the special ratio  $J_{\perp} = 2J_d$ . Hence, it provides a suggestive realization of the model exactly in the quantum critical point predicted in Refs. [8,11]. The contribution to the specific heat from magnetic excitations was fitted with an empirical formula which includes a term linear in  $T$ , characteristic to gapless spinons. Susceptibility and ESR measurements gave no indication for long range order throughout the whole measured temperature range, but indicate a considerable reduction compared to a standard spin-chain system at low  $T$ . The experimental data appear to indicate the existence of a spin-liquid component, that constitutes a fraction of the degrees of freedom in the system.

A more recent study of NOCuNO by Raman scattering<sup>15</sup> indicated that a dynamical interplay between spin and lattice degrees of freedom exists in this material which might lead to novel phases. Moreover, the Debye temperature in NOCuNO is of the same order of magnitude as the spin exchange interactions. It is known that when these two energy scales are comparable then the spin-lattice coupling is enhanced<sup>16,17</sup>. These observations motivate the study of the effect of spin-lattice coupling, which was not considered in earlier theoretical studies of the NT model.

One of the prominent consequences of spin-phonon coupling is the emergence of spin-Peierls (SP) instability. This effect occurs when the exchange couplings are modulated due to distortions in the distance between neighboring atoms, yielding an alternation of strong and weak bonds. The SP instability tends to dimerize the spin-chain, therefore it can destroy the spin-liquid and form a VBC of longitudinal dimers. Away from the critical point of Ref. [8], ( $J_{\perp} = 2J_d$ ), a competition arises

between the SP instability (which tends to create longitudinal dimers) and the transverse exchange coupling (which tends to create transverse dimers). This competition may lead to a phase transition between different types of dimer crystals, or induce a new phase.

In a previous work<sup>11</sup> Starykh and Balents considered a dimer-dimer interaction term which may be generated by higher-order interchain interactions, and studied the influence of this interaction term via a renormalization-group (RG) approach. They showed that various ordered nonmagnetic phases (i.e. with zero magnetization) can form even in the absence of a SP term. The possible phases are two types of VBC, of staggered and columnar longitudinal singlets, in addition to the rung singlets and rung triplets (Haldane phase<sup>18</sup>) VBC states predicted by NT. Later numerical studies [12] confirmed the emergence of such phases for sufficiently strong interchain interactions. This suggests an additional mechanism for SP instability besides interaction with phonons.

In this paper, we examine the effect of the SP instability on the low-energy physics of the NT model. For this purpose we consider a two-leg ladder version of the NT model and introduce a SP instability along the legs as well as XXZ anisotropy of  $J_{\perp}, J_d$ . In the absence of transverse interactions, since the SP instability is strongly relevant, it tends to dimerize the legs of the ladder. This leads to two distinct ground states which differ by the relative sign of the Peierls deformation on the two coupled chains (see Fig. 2). Considering all of the interactions (perpendicular, diagonal and SP) in a Bosonization description, we map the model onto an effective self dual sine-Gordon model which we show is equivalent to a spin-chain in a staggered and tilted magnetic field. Our main result is that the effect of the SP instability on the NT model may lead to a “Plaquette-ordered” state - a crys-

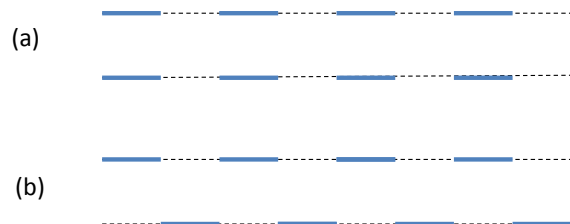


FIG. 2: (color online) Two possible ordering of valence bonds on two noninteracting chains: (a) columnar dimers (CD), (b) staggered dimers (SD). Thick blue lines represent dimers on the stronger bonds.

tal of 4-spins plaquettes where on each plaquette there is a coherent superposition of longitudinal and transverse dimers. There are two types of plaquette ground states corresponding to the two types of dimerized states on the legs. Generically the ground state is gapped and the tuning of parameters [the SP distortion  $\delta J_{\parallel}$ , the inter-leg coupling  $(J_{\perp} - 2J_d)$  and the anisotropies  $J_{\alpha}^z/J_{\alpha}^{xy}$ ] leads to a smooth interpolation between longitudinal and transverse VBC without a second order phase transition. A gapless spin-liquid state can apparently be recovered when the SP deformation is of the type staggered (Fig. 2(b)), under extreme conditions: strong anisotropy of  $J_{\perp}$ ,  $J_d$ , and rung exchange of the order of magnitude of the leg exchange. However, the closing of a gap in the Plaquette-ordered state is always preempted by a *first order* transition to the original VBC of leg-dimers.

The paper is organized as follows: in Sec. II we derive

the low-energy model for the spin system in the presence of a SP instability along the legs of the ladder. In Sec. III we analyze the model and demonstrate the emergence of the Plaquette-order (subsection IIIA) and the phase transition to the VBC state (subsection IIIB). Details of the calculations of dimer correlation functions are discussed in the Appendix. Finally, in Sec. IV, we summarize the results and discuss their possible relevance to the behavior of the 2D realizations of the frustrated coupled chains model.

## II. THE MODEL

We consider a two-leg XXZ ladder version of the NT model (Eq. (2))

$$H_{ladder} = \sum_j \left\{ \sum_{\nu=1,2} \left\{ \frac{J_{\parallel}}{2} [S_{j,\nu}^+ S_{j+1,\nu}^- + H.c.] + J_{\parallel}^z S_{j,\nu}^z S_{j+1,\nu}^z \right\} + \frac{J_{\perp}}{2} [S_{j,1}^+ S_{j,2}^- + H.c.] + J_{\perp}^z S_{j,1}^z S_{j,2}^z + \frac{J_d}{2} [S_{j,1}^+ (S_{j+1,2}^- + S_{j-1,2}^-) + H.c.] + J_d^z S_{j,1}^z (S_{j+1,2}^z + S_{j-1,2}^z) \right\}, \quad (3)$$

with strong intrachain coupling ( $J_{\parallel} \gg J_{\perp}, J_d$ ) and where all exchange couplings are positive. We then introduce a SP instability along the legs of the ladder, described by a contribution to the Hamiltonian of the form

$$H_P^{\sigma} = \frac{\delta J_{\parallel}^{xy}}{2} \sum_j (-)^j [S_{j,1}^+ S_{j+1,1}^- + \sigma S_{j,2}^+ S_{j+1,2}^- + H.c.] + \delta J_{\parallel}^z \sum_j (-)^j [S_{j,1}^z S_{j+1,1}^z + \sigma S_{j,2}^z S_{j+1,2}^z]. \quad (4)$$

This term describes a static deformation of the exchange constants along the legs. In the absence of transverse coupling between the chains 1 and 2, the ground state of each chain is a product of singlets on the strong bonds (i.e., a one-dimensional VBC), with a gap of the order of  $\delta J_{\parallel}$  between the singlet ground state and the lowest triplet excitation. The parameter  $\sigma = \pm$  is the relative sign of the Peierls deformation on the two chains. The SP term is relevant as long as we are away from the ferromagnetic transition point, therefore, in our case, it is strongly relevant and tends to open a gap on each chain independently. As a result, in the case of two uncoupled chains there are two possible patterns in which a VBC can form on the chains, depending on  $\sigma$ :  $\sigma = +$  yields a columnar dimers state (CD) and  $\sigma = -$  a staggered dimers state (SD), as shown in Fig. 2.

To derive the low-energy model of the system, we first use the Jordan-Wigner transformation which maps the spin operators into Fermion fields. In the absence of mag-

netic field the Fermi energy is at the middle of the band, and the Fermion operators can be expressed in terms of Bosonic ones related to the Fermion density fluctuations:

$$\psi_{R/L,\nu} = \frac{1}{\sqrt{2\pi a}} e^{-i(\pm\phi_{\nu} - \theta_{\nu})}, \quad (5)$$

where  $R, L$  stands for right and left moving Fermions, respectively,  $a$  is the lattice constant and  $\nu = 1, 2$  is the leg index. This procedure can be shortly summarized by the following spin to Boson transformation

$$S_{\nu}^+(x) = \frac{e^{-i\theta_{\nu}(x)}}{\sqrt{2\pi a}} [(-)^x + \cos(2\phi_{\nu}(x))], \\ S_{\nu}^z(x) = -\frac{1}{\pi} \partial_x \phi_{\nu}(x) + \frac{(-)^x}{\pi a} \cos(2\phi_{\nu}(x)). \quad (6)$$

We now Bosonize the Hamiltonian  $H = H_{ladder} + H_P$ , starting from

$$H_{ladder} = \int dx \sum_{\nu=1,2} \frac{u}{2\pi} \left[ \frac{1}{K} (\partial_x \phi_{\nu})^2 + K (\partial_x \theta_{\nu})^2 \right] \\ + \int dx \left[ \frac{g}{(2\pi a)^2} \cos(\theta_1 - \theta_2) + \frac{g^z}{(2\pi a)^2} \cos[2(\phi_1 - \phi_2)] \right. \\ \left. + \frac{g^z}{(2\pi a)^2} \cos[2(\phi_1 + \phi_2)] \right] + (J_{\perp}^z + 2J_d^z) a \int dx \frac{\partial_x \phi_1 \partial_x \phi_2}{\pi^2}, \\ g \equiv \frac{2\pi a (J_{\perp} - 2J_d)}{(2\pi a)^2}, \quad g^z \equiv \frac{2\pi a (J_{\perp}^z - 2J_d^z)}{(2\pi a)^2}. \quad (7)$$

Here  $u$  and  $K$  are the Luttinger parameters of each chain on its own and are given by<sup>21</sup>

$$u = \frac{J_{\parallel}}{2} \cdot \frac{\sqrt{1 - (J_{\parallel}^z/J_{\parallel})^2}}{1 + \frac{1}{\pi} \arccos(-J_{\parallel}^z/J_{\parallel})},$$

$$K = \frac{\pi}{2 \arccos(-J_{\parallel}^z/J_{\parallel})}. \quad (8)$$

This part can be written more conveniently in terms of independent symmetric and antisymmetric modes<sup>19-21</sup>

$$\phi_{s/a} = \frac{\phi_1 \pm \phi_2}{\sqrt{2}}, \quad \theta_{s/a} = \frac{\theta_1 \pm \theta_2}{\sqrt{2}}. \quad (9)$$

Then,  $H_{ladder}$  assumes the form

$$H_{ladder} = \int dx \left\{ \sum_{\mu=a,s} \frac{u_{\mu}}{2\pi} \left[ \frac{1}{K_{\mu}} (\partial_x \phi_{\mu})^2 + K_{\mu} (\partial_x \theta_{\mu})^2 \right] \right.$$

$$+ g \cos(\sqrt{2}\theta_a)$$

$$\left. + g^z \cos(\sqrt{8}\phi_a) + g^z \cos(\sqrt{8}\phi_s) \right\} \quad (10)$$

where for  $J_{\perp}, J_d \ll J_{\parallel}$

$$K_{a,s} \cong K [1 \pm \gamma],$$

$$u_{a,s} \cong u [1 \mp \gamma],$$

$$\gamma \equiv \frac{K(J_{\perp}^z + 2J_d^z)a}{2\pi u}. \quad (11)$$

Bosonization of  $H_P^{\sigma}$  (see, e.g., Ref. [21] for a detailed derivation) yields a term more conveniently written in terms of the original fields  $\phi_1, \phi_2$ :

$$H_P^{\sigma} \sim g_P \int dx [\sin(2\phi_1) + \sigma \sin(2\phi_2)],$$

$$g_P \equiv \frac{\delta J_{\parallel}}{\pi a}. \quad (12)$$

Then, substituting Eq. (9) into Eq. (12), recasts  $H_P^{\sigma}$  as a coupling term between the  $a$  and  $s$  sectors. The resulting full Hamiltonian is

$$H = H_{ladder} + H_P^{\sigma} = H_a + H_s + H_{as}^{\sigma},$$

$$H_a = \frac{u_a}{2\pi} \int dx \left[ \frac{1}{K_a} (\partial_x \phi_a)^2 + K_a (\partial_x \theta_a)^2 \right] + g \int dx \cos(\sqrt{2}\theta_a) + g^z \int dx \cos(\sqrt{8}\phi_a),$$

$$H_s = \frac{u_s}{2\pi} \int dx \left[ \frac{1}{K_s} (\partial_x \phi_s)^2 + K_s (\partial_x \theta_s)^2 \right] + g^z \int dx \cos(\sqrt{8}\phi_s),$$

$$H_{as}^{\sigma} = g_P \int dx [\sin[\sqrt{2}(\phi_s + \phi_a)] + \sigma \sin[\sqrt{2}(\phi_s - \phi_a)]]. \quad (13)$$

Note that at the critical point of the NT model, which for anisotropic rung coupling requires both  $J_{\perp} = 2J_d$  and  $J_{\perp}^z = 2J_d^z$ , the coefficients  $g, g^z$  in Eq. (13) vanish. However, away from the critical point we must consider the competition between all the cosine terms appearing. The relevance of the terms is determined by the scaling dimensions. Let us denote by  $d_{a/s}^z$  the scaling dimensions of the terms  $g^z \cos(\sqrt{8}\phi_{a/s})$  respectively in the  $a/s$  sector,  $d$  of the term with coefficient  $g$ , and  $d_P$  the scaling dimension of the term with coefficient  $g_P$ . Employing a perturbative RG, these scaling dimensions are given by

$$d = \frac{1}{2K_a}, \quad d_a^z = 2K_a, \quad d_P = \frac{1}{2}(K_a + K_s), \quad d_s^z = 2K_s. \quad (14)$$

Since  $\gamma$  (Eq. (11)) is positive,  $d_s^z < d_a^z$ . Therefore  $g^z \cos(\sqrt{8}\phi_a)$  is always the least relevant term, and will be neglected henceforth. Comparing  $d_P$  and  $d_s^z$  we find that for weak rung coupling ( $\gamma < 1/2$ ), the  $g_P$  term is also

more relevant than the  $g^z \cos(\sqrt{8}\phi_s)$  term. This analysis of the scaling dimensions leads to the conclusion that for weak rung coupling the dominant terms which govern the low energy description are the  $g$  and  $g_P$  terms, which indicate a potential competition between the Peierls instability (which tends to form leg-dimers) to the rung coupling (which tends to form rung-dimers for  $g > 0$ ). There is a special value of  $K$  for which the scaling dimensions of the most relevant terms are equal: from Eqs. (11), (14) we find  $d = d_P$  for

$$K^* = \frac{1}{\sqrt{2(1+\gamma)}} \cong \frac{1}{\sqrt{2}}. \quad (15)$$

We now recall that for arbitrary  $K$  in the regime of interest  $1/2 \leq K \leq 1$  (i.e.  $0 < J_{\parallel}^z \leq J_{\parallel}$ ),  $K_s < 1$  hence the term  $g^z \cos(\sqrt{8}\phi_s)$  is also relevant, and tends to lock the value of the symmetric field  $\phi_s$ . This affects the interaction term  $H_{as}^{\sigma}$  which has a different form for

SD ( $\sigma = -$ ) and CD ( $\sigma = +$ ) configurations:

$$\begin{aligned} H_{as}^+ &= 2g_P \int dx \sin(\sqrt{2}\phi_s) \cos(\sqrt{2}\phi_a), \\ H_{as}^- &= 2g_P \int dx \cos(\sqrt{2}\phi_s) \sin(\sqrt{2}\phi_a). \end{aligned} \quad (16)$$

In a semiclassical approximation, the  $\cos(\sqrt{8}\phi_s)$  term in Eq. (13) obtains a finite expectation value which mini-

mizes  $H_s$ :

$$\langle \cos(\sqrt{8}\phi_s) \rangle \cong -1 \Rightarrow \sqrt{2}\langle \phi_s \rangle \cong \pi/2. \quad (17)$$

We can therefore replace  $\phi_s$  with its expectation value everywhere it appears in the interaction term  $H_{as}^\sigma$ . For  $\sigma = +$ , in this semi-classical approach, we obtain an effective Hamiltonian for the anti-symmetric mode  $\phi_a$

$$H_a^{eff} = \int dx \left\{ \frac{u_a}{2\pi} \left[ \frac{1}{K_a} (\partial_x \phi_a)^2 + K_a (\partial_x \theta_a)^2 \right] + g \cos(\sqrt{2}\theta_a) + 2g_P \cos(\sqrt{2}\phi_a) \right\}, \quad (18)$$

where the last term results from the substitution  $\sin(\sqrt{2}\phi_s) \cong \sin(\sqrt{2}\langle \phi_s \rangle) = 1$  in  $H_{as}^+$  [Eq.(16)].  $H_a^{eff}$  belongs to a class of self dual sine-Gordon models which have known solutions<sup>22</sup>. This will be analyzed in detail in the next section, and will be shown to yield a gapped, plaquette-ordered ground state. However for  $\sigma = -$ , this naive semiclassical approximation would result in  $H_{as}^- = 0$ , since  $\cos(\sqrt{2}\phi_s) \cong \cos(\sqrt{2}\langle \phi_s \rangle) = 0$ . This would imply that the SP instability is completely suppressed, and by tuning  $g$  to zero one recovers a gapless Luttinger liquid state in the antisymmetric sector. Since  $H_P^\sigma = H_{as}^\sigma$  is strongly relevant, it seems improbable that it can vanish completely from the low energy theory; rather, this is an artefact of the naive assumption  $\langle \cos(\sqrt{8}\phi_s) \rangle = -1$ . However, quantum fluctuations generally induce a finite expectation value which may be different than  $-1$ , in which case  $H_{as}^-$  does not vanish. In the next section we discuss its contribution more carefully.

### III. PHASE DIAGRAM

In what follows we focus on the properties of the model for  $K \sim K^* \approx 1/\sqrt{2}$ , in which, as noted in the previous section, the terms responsible for the formation of leg and rung singlets are equally relevant. We derive a general

theory that accounts for both the SD and CD configurations of the SP instability, given in terms of an effective Hamiltonian similar in form to Eq. (18). As we show below, this effective model indicates the potential formation of a ‘‘Plaquette order’’ phase.

#### A. Emergence of Plaquette Order

In order to simplify the Hamiltonian of Eq. (13), we define new Bosonic fields via the transformation

$$\begin{aligned} \phi_p &= \phi_s + \tau\phi_a, \quad \theta_p = \tau\theta_a, \\ \phi_f &= \sqrt{2}\phi_s, \quad \theta_f = \frac{1}{\sqrt{2}}(\theta_s - \tau\theta_a) \end{aligned} \quad (19)$$

with  $\tau = \pm 1$ , which preserve the canonical commutation relations

$$[\phi_p(x), \theta_p(x')] = [\phi_f(x), \theta_f(x')] = i\pi \text{sign}(x - x'). \quad (20)$$

Note that from Eq. (9),  $\phi_p$  and  $\theta_f$  are simply related to the original fields  $\phi_\nu, \theta_\nu$ : for  $\tau = +$ ,  $\phi_p = \sqrt{2}\phi_1$  and  $\theta_f = \theta_2$ , and for  $\tau = -$  the roles of 1, 2 are interchanged. Thus the index  $\tau$  encodes a breaking of reflection symmetry across the ladder. Substituting Eq. (19) in Eq. (13) and removing the least relevant term  $\cos(\sqrt{8}\phi_a)$ , we get

$$\begin{aligned}
H &= H_p^\sigma + H_f + H_{pf}^\sigma \\
H_p^\sigma &= \frac{u_p}{2\pi} \int dx \left[ \frac{1}{K_p} (\partial_x \phi_p)^2 + K_p (\partial_x \theta_p)^2 \right] + g \int dx \cos(\sqrt{2}\theta_p) + g_P (\delta_{\tau,-\sigma} + \sigma \delta_{\tau,\sigma}) \int dx \sin(\sqrt{2}\phi_p), \\
H_f &= \frac{u_f}{2\pi} \int dx \left[ \frac{1}{K_f} (\partial_x \phi_f)^2 + K_f (\partial_x \theta_f)^2 \right] + g^z \int dx \cos(2\phi_f), \\
H_{pf}^\sigma &= \int dx \left\{ -\frac{\sqrt{2}u_a}{K_a} \partial_x \phi_f \partial_x \phi_p + 2\sqrt{2}u_s K_s \partial_x \theta_f \partial_x \theta_p + g_P (\delta_{\tau,\sigma} + \sigma \delta_{\tau,-\sigma}) [\sin(2\phi_f) \cos(\sqrt{2}\phi_p) - \cos(2\phi_f) \sin(\sqrt{2}\phi_p)] \right\}.
\end{aligned} \tag{21}$$

Here the velocities are given by

$$\begin{aligned}
u_p &= u_a \sqrt{\frac{u_a K_a + u_s K_s}{u_a K_a}} \cong \sqrt{2}u(1 - \gamma), \\
u_f &= \sqrt{u_s K_s \left( \frac{u_a}{K_a} + \frac{u_s}{K_s} \right)} \cong \sqrt{2}u
\end{aligned} \tag{22}$$

and the Luttinger parameters are

$$\begin{aligned}
K_p &= \sqrt{\frac{K_a(u_a K_a + u_s K_s)}{u_a}} \cong \sqrt{2}K(1 + \gamma), \\
K_f &= \sqrt{\frac{4u_s K_s^2 K_a}{u_a K_s + u_s K_a}} \cong \sqrt{2}K,
\end{aligned} \tag{23}$$

where in the final approximations we neglect terms of order  $\gamma^2$ .

Next we show that for  $K \cong 1/\sqrt{2}$  such that  $K_f \cong 1$ , the  $f$  sector reduces to a model of gapped free Fermions. Using Eq. (5) (with  $\phi_\nu, \theta_\nu$  replaced by  $\phi_f, \theta_f$ ), the cosine term in  $H_f$  can be reformionized to give

$$\cos(2\phi_f) = \pi a (\psi_R^\dagger \psi_L + \psi_L^\dagger \psi_R). \tag{24}$$

Reformionizing the first term of  $H_f$  as well and transforming to momentum space we obtain

$$\begin{aligned}
H_f &= \sum_k u_f k (c_{R,k}^\dagger c_{R,k} - c_{L,k}^\dagger c_{L,k}) + \Delta \sum_k (c_{R,k}^\dagger c_{L,k} + c_{L,k}^\dagger c_{R,k}), \\
\Delta &\equiv \pi a g^z.
\end{aligned} \tag{25}$$

This Hamiltonian can be diagonalized by a Bogoliubov transformation<sup>21</sup>

$$\begin{aligned}
c_{+,k}^\dagger &= \alpha_k c_{R,k}^\dagger + \beta_k c_{L,k}^\dagger, \\
c_{-,k}^\dagger &= -\beta_k c_{R,k}^\dagger + \alpha_k c_{L,k}^\dagger,
\end{aligned} \tag{26}$$

with

$$\begin{aligned}
\alpha_k &= \frac{1}{\sqrt{2}} \left[ 1 + \frac{u_f k}{\sqrt{(u_f k)^2 + \Delta^2}} \right]^{1/2}, \\
\beta_k &= \frac{1}{\sqrt{2}} \left[ 1 - \frac{u_f k}{\sqrt{(u_f k)^2 + \Delta^2}} \right]^{1/2},
\end{aligned} \tag{27}$$

after which  $H_f$  becomes

$$\begin{aligned}
H_f &= \sum_k \sum_{\nu=\pm} E_{\nu,k} c_{\nu,k}^\dagger c_{\nu,k}, \\
E_{\pm,k} &= \pm \sqrt{(u_f k)^2 + \Delta^2}.
\end{aligned} \tag{28}$$

Now, using the fact that  $H_f$  describes gapped free Fermions, for low  $T \ll \Delta$  we can simplify the interaction term  $H_{pf}$  by a mean-field approximation. This amounts to replacing  $\cos 2\phi_f$  as well as  $\partial_x \phi_f$ ,  $\partial_x \theta_f$  and  $\sin 2\phi_f$  in  $H_{pf}^\sigma$  [Eq. (21)] by their expectation values. In terms of Fermionic fields these operators give

$$\begin{aligned}
\sin 2\phi_f &= -i\pi a (\psi_R^\dagger \psi_L - H.c.), \\
\partial_x \phi_f &= -\pi (\psi_R^\dagger \psi_R + \psi_L^\dagger \psi_L), \\
\partial_x \theta_f &= -\pi (\psi_R^\dagger \psi_R - \psi_L^\dagger \psi_L).
\end{aligned} \tag{29}$$

Fourier transforming and using Eq. (26), we get (to leading order in  $\frac{\Delta a}{u_f}$ )

$$\langle \sin 2\phi_f \rangle = 0, \langle \partial_x \phi_f \rangle = 0, \langle \partial_x \theta_f \rangle = 0,$$

$$O_f \equiv \langle \cos 2\phi_f \rangle = \pi a \langle \psi_R^\dagger \psi_L + \psi_L^\dagger \psi_R \rangle = \sum_k \{ \alpha_k \beta_k \langle c_{+,k}^\dagger c_{+,k} - c_{-,k}^\dagger c_{-,k} \rangle + (\alpha_k^2 - \beta_k^2) \langle c_{+,k}^\dagger c_{-,k} + c_{-,k}^\dagger c_{+,k} \rangle \}, \quad (30)$$

which yields

$$O_f \sim -\frac{|\Delta|}{u_f/a} \ln \left[ \frac{u_f/a}{|\Delta|} \right]. \quad (31)$$

Here we have used  $\langle c_{\mu,k}^\dagger c_{\nu,k'} \rangle = \delta_{\mu\nu} \delta_{k,k'} f_{\mu,k}$  (for  $\mu, \nu = \pm$ ), with  $f_{\pm,k} = (1 + e^{E_{\pm,k}/T})^{-1}$  the Fermi distribution function, approximated by  $f_- \approx 1$ ,  $f_+ \approx 0$  for  $T \ll \Delta$ . Substituting back into Eq. (21), this yields an effective Hamiltonian for the  $p$  sector:

$$\begin{aligned} H_p^{\sigma,eff} &= \frac{u_p}{2\pi} \int dx \left[ \frac{1}{K_p} (\partial_x \phi_p)^2 + K_p (\partial_x \theta_p)^2 \right] \\ &+ g \int dx \cos(\sqrt{2}\theta_p) + \tilde{g}_P(\sigma, \tau) \int dx \sin(\sqrt{2}\phi_p), \\ \tilde{g}_P(\sigma, \tau) &\equiv (\delta_{\tau,-\sigma} + \sigma \delta_{\tau,\sigma}) g_P [1 - \sigma O_f]. \end{aligned} \quad (32)$$

The SP configuration on the ladder, CD ( $\sigma = +$ ) or SD ( $\sigma = -$ ) is encoded in the effective Hamiltonian Eq. (32) by the parameter  $\tilde{g}_P(\sigma, \tau)$ . Its dependence on  $\sigma, \tau$  reflects a crucial distinction between the two SP configurations: first, in the CD case this effective parameter is symmetric,  $\tilde{g}_P(+, +) = \tilde{g}_P(+, -)$ ;

i.e., the model is identical for  $\tau = \pm$ . In contrast, the SD configuration yields  $\tilde{g}_P(-, +) = -\tilde{g}_P(-, -)$ , namely two distinct Hamiltonians for  $\tau = \pm$ . Second, since  $O_f < 0$  [see Eq.(31)],  $\tilde{g}_P(+, \tau)$  is always finite and obeys  $|\tilde{g}_P(+, \tau)| > |\tilde{g}_P(-, \tau)|$ . Most prominently, only in the SD case ( $\sigma = -$ ) a spin liquid phase can be reached. This occurs for very special values of the exchange interactions where *both*  $g$  and  $\tilde{g}_P(-, \tau)$  vanish: when  $J_\perp^{xy} = 2J_d^{xy}$  (i.e., at the critical point of the NT model), and at the same time  $J_\perp \sim J_\parallel$  so that  $O_f \sim 1$  [23]. Then all the interaction terms vanish and we are left with a Luttinger-liquid model. For this extremely-fine-tuned point, this analysis gives a Luttinger liquid phase in the case where the SP instability on the legs of the ladder is of the SD type (Fig 2(b)). This Luttinger liquid then describes gapless spinons on a single chain composed of the interlaced chains 1 and 2. We note, however, that under these conditions another ordered ground state is likely to be favored, as will be discussed in subsection B.

To explore the more generic case where  $g$  and/or  $\tilde{g}_P$  are finite, we next rescale the fields,  $\tilde{\phi}_p = \frac{\phi_p}{\sqrt{2}}$ ,  $\tilde{\theta}_p = \sqrt{2}\theta_p$ , and accordingly the Luttinger parameter  $\tilde{K}_p = \frac{K_p}{2}$  to obtain

$$H^{eff} = \int dx \left\{ \frac{u_p}{2\pi} \left[ \frac{1}{\tilde{K}_p} (\partial_x \tilde{\phi}_p)^2 + \tilde{K}_p (\partial_x \tilde{\theta}_p)^2 \right] + g \cos(\tilde{\theta}_p) + \tilde{g}_P(\sigma) \sin(2\tilde{\phi}_p) \right\}. \quad (33)$$

For  $g > 0$  the interaction terms  $\cos(\tilde{\theta}_p)$ ,  $\sin(2\tilde{\phi}_p)$  are dimerization operators, each one creates different dimers: the  $\cos(\tilde{\theta}_p)$  creates dimers along the rungs of the ladder, and  $\sin(2\tilde{\phi}_p)$  creates dimers along the legs of the ladder.

It is convenient to define  $\tilde{\phi} = \tilde{\phi}_p - \pi/4$ , so that  $\sin(2\tilde{\phi}_p) = \cos(2\tilde{\phi})$ , and we arrive at a self-dual sine-Gordon model

$$H^{eff} = \int dx \left\{ \frac{u_p}{2\pi} \left[ \frac{1}{\tilde{K}_p} (\partial_x \tilde{\phi})^2 + \tilde{K}_p (\partial_x \tilde{\theta})^2 \right] + g \cos(\tilde{\theta}) + \tilde{g}_P(\sigma, \tau) \cos(2\tilde{\phi}) \right\}. \quad (34)$$

This is a special case of a series of models reviewed in Ref. [22]. In our case the choice  $K \sim 1/\sqrt{2}$  dictates  $K_p \sim 1$  and hence  $\tilde{K}_p \sim 1/2$ , i.e. the quadratic part of the model

is at the Heisenberg point, which is invariant under spin

rotations. Then, we use the following relations

$$\begin{aligned}\cos(\tilde{\theta}) &\sim (-)^x \sigma_x, \\ \cos(2\tilde{\phi}) &\sim (-)^x \sigma_z,\end{aligned}\quad (35)$$

where the  $\sigma_a$  operators are pauli matrices representing fictitious local spins. The resulting (fictitious) spin model is

$$\begin{aligned}H &= \sum_i [J\sigma_i \cdot \sigma_{i+1} + (-)^x \mathbf{B} \cdot \sigma_i], \\ \mathbf{B} &= \tilde{g}_P(\sigma, \tau) \hat{z} + g \hat{x}.\end{aligned}\quad (36)$$

Eq. (36) describes a spin-chain model in a staggered magnetic field in the  $z-x$  plane, at an angle

$$\alpha = \arctan(g/\tilde{g}_P(\sigma, \tau)) \quad (37)$$

from the  $\hat{z}$  direction. Now we rotate the coordinate system so that the field will be in the  $\hat{z}$  direction:

$$\begin{aligned}\hat{x}' &= \cos \alpha \hat{x} - \sin \alpha \hat{z}, \\ \hat{z}' &= \sin \alpha \hat{x} + \cos \alpha \hat{z}.\end{aligned}\quad (38)$$

The  $\sigma_a$  spins are then related to the rotated spins  $\sigma'_a$  by

$$\begin{aligned}\sigma_x &= \sigma'_x \cos \alpha + \sigma'_z \sin \alpha, \\ \sigma_z &= \sigma'_z \cos \alpha - \sigma'_x \sin \alpha.\end{aligned}\quad (39)$$

After this rotation the model is mapped onto a spin-chain in a staggered magnetic field along the  $\hat{z}$  direction, which in Bosonization gives a regular sine-Gordon model with rotated fields  $\phi'$ ,  $\theta'$ :

$$\begin{aligned}H &= \int dx \left\{ \frac{u'}{2\pi} \left[ \frac{1}{K'} (\partial_x \phi')^2 + K' (\partial_x \theta')^2 \right] + g' \cos(2\phi') \right\}, \\ g' &\equiv \sqrt{\tilde{g}_P^2(\sigma, \tau) + g^2}, \quad u' = \tilde{u}_p = u_p, \quad K' = \tilde{K}_p = K_p/2.\end{aligned}\quad (40)$$

The  $\cos(2\phi')$  term opens a gap  $\Delta'$  and obtains a finite expectation value. This term is also the order parameter of this model. Recalling that  $K' \sim 1/2$ , the system is deep in the gapped phase where a semi-classical approximation is justified to evaluate  $\Delta'$ . A variational calculation (see, e.g., Ref. [21] for details) yields

$$\Delta' \sim u' \Lambda \left( \frac{K' g'}{u' \Lambda^2} \right)^{1/(2-K')} \quad (41)$$

with  $\Lambda \sim 1/a$ . The expectation value of the order parameter is subsequently given by

$$\langle \cos 2\phi' \rangle \sim - \left( \frac{g'}{u' \Lambda^2} \right)^{K'} \sim - \left( \frac{\Delta'}{u' \Lambda} \right)^{(2-K')K'}. \quad (42)$$

Substituting  $K' = 1/2$ , this yields

$$\Delta' \sim u' \Lambda \left( \frac{g'}{u' \Lambda^2} \right)^{2/3}, \quad \langle \cos 2\phi' \rangle \sim - \left( \frac{g'}{u' \Lambda^2} \right)^{1/2}. \quad (43)$$

Note that generically  $g' > g, \tilde{g}_P(\sigma, \tau)$ ; rather than competing with each other, the two self-dual interaction terms in Eq. (34) cooperate to form an ordered ground state which smoothly evolves upon tuning of the parameters, and there is no phase transition.

Using Eqs. (35), (37) and (39) we express the order parameter field in terms of the fields  $\tilde{\phi}$  and  $\tilde{\theta}$

$$\begin{aligned}O_p &\equiv \cos(2\phi') = \cos \alpha \cos(2\tilde{\phi}) + \sin \alpha \cos(\tilde{\theta}), \\ \cos \alpha &= \frac{\tilde{g}_P(\sigma, \tau)}{\sqrt{\tilde{g}_P^2(\sigma, \tau) + g^2}}, \quad \sin \alpha = \frac{g}{\sqrt{\tilde{g}_P^2(\sigma, \tau) + g^2}}.\end{aligned}\quad (44)$$

In both the CD ( $\sigma = +$ ) and SD ( $\sigma = -$ ) configurations, the ground state spontaneously breaks reflection symmetry across the ladder, with two distinct ground states (labeled by  $\tau = \pm$ ) of identical energies. To understand the physical interpretation of these ordered states, recall that  $\cos(2\tilde{\phi})$  and  $\cos(\tilde{\theta})$  create longitudinal (leg) and transverse (rung) dimers, respectively. Hence Eq. (44) implies that the order parameter is an entangled superposition of longitudinal and transverse dimers, on plaquettes of four spins. The ground state is a crystal of such plaquettes, as illustrated in Fig. 3. Since the dimers on chains 1,2 have two possible configurations, CD and SD, the plaquettes also have two possible ordered states, closed and open rectangular plaquettes, corresponding to the CD and SD states respectively. The open rectangular plaquette order is relatively fragile, and under extreme conditions where  $g' = 0$ , a gapless spin-liquid can be recovered. In comparison, the closed rectangular order is more robust and is lower in energy for given strength of the exchange interactions.

The long range order of dimers on distant plaquettes is confirmed by the calculation of dimer-dimer correlation functions, which do not decay with increasing distance (the details of the calculation are given in the appendix). For  $T \ll \Delta'$  and  $x \gg \xi$ , where  $\xi = u'/\Delta'$  is the correlation length, these are given by constant asymptotic values

$$\begin{aligned}\chi_{ll}(x \gg \xi) &\cong \cos^2(\alpha) (\Lambda \xi)^{-2K'}, \\ \chi_{tt}(x \gg \xi) &\cong \sin^2(\alpha) (\Lambda \xi)^{-2K'}, \\ \chi_{lt}(x \gg \xi) &\cong \frac{1}{2} \sin(2\alpha) (\Lambda \xi)^{-2K'}.\end{aligned}\quad (45)$$

Here

$$\chi_{\mu\nu}(x, t) \equiv \langle \epsilon_\mu(x, t) \epsilon_\nu(0, 0) \rangle, \quad (\mu, \nu = l, t) \quad (46)$$

where  $\epsilon_l, \epsilon_t$  denote longitudinal and transverse dimer operators, respectively (see App. A). In particular, the long-range nature of  $\chi_{lt}$ , describing the correlation between a longitudinal and a transverse dimer, indicates the entanglement between two types of dimers within a plaquette.



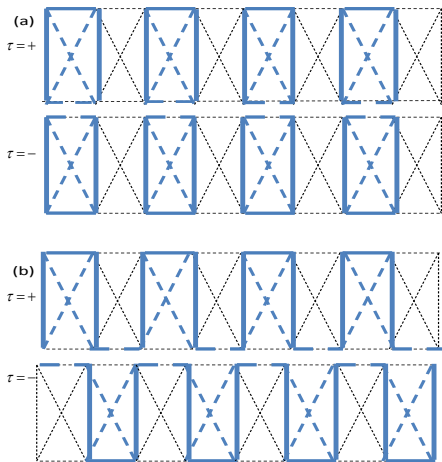


FIG. 3: (color online) Two possible types of plaquette order on the frustrated SP ladder: (a) closed plaquettes corresponding to  $\sigma = +$ , (b) open plaquettes corresponding to  $\sigma = -$ . Thick solid blue lines represent strong dimers, and thick dashed blue lines represent weakened dimers. In each case, two distinct plaquette-ordered ground-state configurations emerge (corresponding to  $\tau = \pm$ ), with spontaneously broken reflection symmetry.

### B. Phase Transition From VBC to Plaquette Order

The calculation presented in subsection A suggests that away from the NT quantum critical point, and particularly for sufficient XXZ anisotropy of the rung coupling, the competition between the transverse and longitudinal (SP) dimerization terms may give rise to an ordered state of Plaquette dimers. However, since the SP term is strongly relevant, as long as  $g_P$  is still relatively large the ground state will be dominated by the SP term, and a VBC state (as depicted in Fig. 2) will likely be favorable. This is especially notable in the case of the SD configuration ( $\sigma = -$ ), where the Plaquette order is partially frustrated. When  $g$  and  $g_P$  are comparable, a first order transition from the VBC order to the plaquette order may occur, tuned by the ratio of  $g$  and  $g_P$ . The transition line in the phase diagram, given in terms of the parameters  $g$  and  $g_P$ , can be derived from energy considerations. To this end, we calculate the gain in energy for each phase to form, and compare them. The energy gain of a massive phase due to a relevant operator is given by the condensation energy

$$\delta E \sim -\frac{\Delta^2}{E_0} \quad (47)$$

where  $\Delta$  is the gap, and  $E_0 = u\Lambda$  (with  $u$  the typical velocity) the high energy cutoff. Similarly to the derivation of Eq. (41) for the gap in the plaquette ordered state, we employ a variational approach to evaluate the gap opened by all relevant operators in terms of the parameters  $g_P$

and  $g^z$ . This gives

$$\begin{aligned} \Delta^z &\sim u_s \Lambda \left( \frac{K_s g^z}{u_s \Lambda^2} \right)^{\frac{1}{2-2K_s}}, \\ \Delta_P &\sim u \Lambda \left( \frac{K g_P}{u \Lambda^2} \right)^{\frac{1}{2-K}}, \end{aligned} \quad (48)$$

where  $\Delta^z$  is the gap opened by  $g^z \cos(\sqrt{8}\phi_s)$  of Eq. (13) and  $\Delta_P$  the gap opened by the original SP term  $H_P^z$  [Eq. (12)]. Using these expressions we can calculate the gain in energy for the competing phases due to these operators. Forming a plaquette order will benefit the energy due to the gap  $\Delta'$  and the energy due to the gap  $\Delta^z$ . Forming a VBC state will benefit the energy due to the gap opened by the SP instability, that is, twice (counted once for each chain) the energy gain from  $\Delta_P$ . Therefore we obtain the overall gain in energy for the competing phases to form:

$$\begin{aligned} \delta E_{\text{plaq}} &= -(\Delta')^2/u' - (\Delta^z)^2/u_s, \\ \delta E_{\text{VBC}} &= -2(\Delta_P)^2/u. \end{aligned} \quad (49)$$

A transition between VBC order and plaquette order occurs when  $\delta E_{\text{plaq}} = \delta E_{\text{VBC}}$ . Using Eqs. (40), (41), (48) and (49) we plot a phase diagram for the transition from VBC order to plaquette order as a function of the strength of the rung dimerization  $g$  and the leg dimerization  $g_P$  for constant  $g^z$ . The result is presented in Fig. 4.

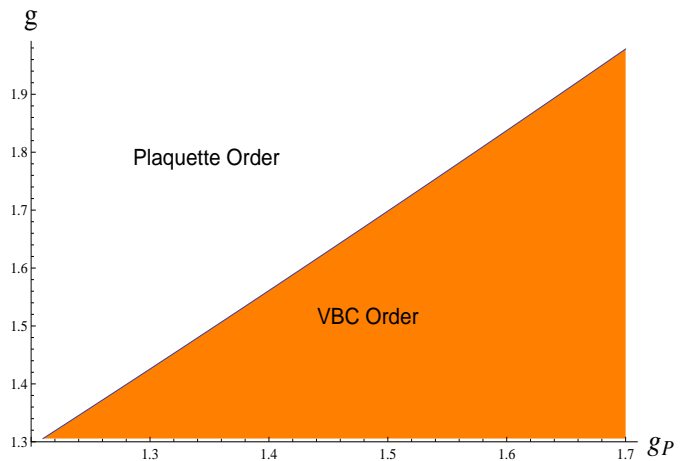


FIG. 4: (color online)  $g-g_P$  phase diagram in arbitrary units for fixed  $g^z = 1.5$ ,  $\sigma = -$ ,  $K = 1/\sqrt{2}$ ,  $\gamma = 0.1$ ,  $u = 6.15$  and  $\Lambda = \pi$ . The phase boundary line denotes a first order transition.

## IV. SUMMARY AND DISCUSSION

We studied a model for a frustrated spin-Peierls ladder, namely a two-leg ladder version of the anisotropic

NT model<sup>8</sup> in the presence of a SP instability on the legs. Two types of SP configurations were considered: columnar dimers (CD) and staggered dimers (SD), which are respectively even and odd under reflection across the ladder (see Fig. 2). The effect of rung exchange interactions ( $J_{\perp}$ ,  $J_d$ ) on the two configurations is distinct; for instance, effectively antiferromagnetic rung coupling ( $J_{\perp} - 2J_d > 0$ ) strengthens the ordering due to a CD instability while it frustrates the SD configuration (and the reverse for  $J_{\perp} - 2J_d < 0$ ). We particularly focus on the case of an intermediate anisotropy on the legs of the ladder where the Luttinger parameter  $K \approx 1/\sqrt{2}$  [i.e.  $J_{\parallel}^z/J_{\parallel} \approx 0.6$  - see Eq. (8)], in which the SP dimerization terms and the rung interactions are equally relevant. By mapping the resulting effective model to a spin-chain in a staggered magnetic field, we found that the interplay between these interactions tends to form a ‘‘Plaquette-ordered’’ phase: a crystal of valence bonds plaquettes where reflection symmetry across the ladder is spontaneously broken (see Fig. 3). The order parameter in this phase is a coherent superposition of longitudinal and transverse dimers, hence all types of dimer-dimer correlations are long-range.

The analysis leading to the above result relies on a mean-field approximation, justified when the rung exchange is tuned far enough from the NT quantum critical point  $J_{\perp} = 2J_d$ . The resulting gap to excitations is smaller in one of the SP configurations (e.g., for  $(J_{\perp} - 2J_d) > 0$  it is the SD configuration), and can even be tuned to zero for an extreme limit of the parameters. Under these extreme conditions, one apparently expects the formation of a gapless, Luttinger liquid mode (which can be interpreted as spin-1/2 chain meandering between the two legs of the ladder). Note that for more generic parameters, quantum fluctuations not accounted for in our low-energy approximations might also soften the gap: these introduce dynamics of the isospin  $\tau$ , and consequently drive an Ising transition. However, typically a gapless liquid state is unstable to other forms of order. In particular, for sufficiently strong SP instability (of either the CD or SD type), the Plaquette-ordered phase always gives way to the VBC state (i.e. a dimer-crystal of the corresponding structure) via a *first order* transition. A typical phase diagram is depicted in Fig. 4.

It should be noted that while the analysis presented in the previous sections, which has focused on a special value of the leg-anisotropy ( $K = 1/\sqrt{2}$ ) allowing the exact mappings to free Fermions and the Heisenberg chain in a staggered field, the conclusions are more general. The formation of a Plaquette ordering essentially arises from the interplay of two highly relevant dimerization interactions, when their gap scales (as calculated for each interaction independently) are comparable. Deviations from  $K = 1/\sqrt{2}$  will thus lead to quantitative rather than qualitative corrections of our main results.

As a final remark, it is suggestive that our findings for the two-leg ladder version of the NT model are the key to

understanding the behavior in physical realizations of the full-fledged 2D model such as the compound NOCuNO studied in Ref. 14. Similarly to the CD and SD instabilities introduced in this paper, in a multi-chain system a variety of lattice distortions generated by the softening of certain phonon modes may occur. This is especially expected in the presence of strong spin-phonon coupling. The resulting interplay between leg and rung dimerization interactions may give rise to various ordered states involving a superposition of transverse and longitudinal dimers, as generalizations of the Plaquette-ordered phase discussed in this paper. Moreover, several distinct broken symmetry states with identical or comparable energy may compete. As a consequence, one generically expects the formation of domains with different ordered spin-gapped configurations. The boundaries between domains can potentially support gapless spin-liquid modes. This would be manifested as a partial spin-liquid contribution to thermodynamic coefficients, as observed in the experiment<sup>14</sup>.

### Acknowledgments

We thank L. Balents, R. Chandra, D. Podolsky, R. Santos and A. Tsvelik, and especially A. Vasiliev and O. Volkova for illuminating discussions. E. S. is grateful to the hospitality of the Aspen Center for Physics (NSF grant 1066293) and to the Simons Foundation. This work was supported by the Israel Science Foundation (ISF) grant 599/10.

### Appendix A: Dimer Correlation Functions

We are interested in the correlations between dimers of spins in the Plaquette ordered state. To this end, we define the dimerization operators

$$\begin{aligned}\epsilon_l &= S_{i,\nu}^+ S_{i+1,\nu}^- - S_{i,\nu}^- S_{i+1,\nu}^+ \quad (\nu = 1, 2), \\ \epsilon_t &= S_{i,1}^+ S_{i,2}^- + S_{i,1}^- S_{i,2}^+, \end{aligned} \quad (\text{A1})$$

where the indices  $l, t$  stand for longitudinal and transverse dimers respectively. Employing Bosonization [Eq. 6], we obtain the following expressions:

$$\epsilon_l \sim \cos(2\tilde{\phi}), \quad \epsilon_t \sim \cos(\tilde{\theta}) \quad (\text{A2})$$

where  $\tilde{\phi}, \tilde{\theta}$  are the fields appearing in Eq. (34) and are defined in the main text. After the rotation of Eq. (39), we get

$$\begin{aligned}\epsilon_l &\sim \cos(2\phi') \cos \alpha - \cos(\theta') \sin \alpha, \\ \epsilon_t &\sim \cos(\theta') \cos \alpha + \cos(2\phi') \sin \alpha. \end{aligned} \quad (\text{A3})$$

The correlation functions between dimers are defined as

$$\chi_{\mu\nu}(x, t) = \langle \epsilon_{\mu}(x, t) \epsilon_{\nu}(0, 0) \rangle, \quad (\mu, \nu = l, t). \quad (\text{A4})$$

Using Eq. (A3), we thus obtain expressions for  $\chi_{\mu\nu}(x, t)$  in terms of correlation functions of two types of operators:  $\cos(2\phi')$  and  $\cos(\theta')$ .

In order to calculate correlation functions of the sine-Gordon model, we use the fact that in the gapped phase the cosine term can be expanded around the average value of  $\phi'$ , so that  $\cos(2\phi') \cong 2(\phi' - \pi/2)^2 - 1$ . Then, changing to a new field  $\varphi = \phi' - \pi/2$ , we arrive at a quadratic Hamiltonian for the massive field  $\varphi$

$$H = \frac{u'}{2\pi} \int dx \left[ \frac{1}{K'} (\partial_x \varphi)^2 + K' (\partial_x \theta')^2 + \frac{(\Delta')^2}{K' (u')^2} \varphi^2 \right], \quad (\text{A5})$$

with the gap  $\Delta'$  given by Eq. (41). The correlation functions of a Gaussian theory can be readily calculated using the methods shown in appendix C of Ref. [21]. The correlations of the form  $\langle \cos(\theta'(x, t)) \cos(\theta'(0)) \rangle$  decay exponentially because due to the uncertainty principle, when  $\phi'$  is ordered,  $\theta'$  fluctuates. Therefore, at  $T \ll \Delta'$  the only contributions to  $\chi_{\mu\nu}(x, t)$  arise from the correlation function

$$C_\varphi(\mathbf{r}) \equiv \langle \cos(2\varphi(\mathbf{r}) + \pi) \cos(2\varphi(0) + \pi) \rangle \sim e^{-2K' G_\varphi(\mathbf{r})} \quad (\text{A6})$$

where the propagator  $G_\varphi(\mathbf{r}) \equiv \langle (\varphi(\mathbf{r}) - \varphi(0))^2 \rangle$  is given by

$$G_\varphi(\mathbf{r}) = \frac{1}{\beta\Omega} \sum_{\mathbf{q}} [1 - \cos(kx + \omega_n \tau)] \frac{2\pi u'}{\omega_n^2 + (u'k)^2 + (\Delta')^2}; \quad (\text{A7})$$

here  $\mathbf{r} = (x, u'\tau)$  with  $\tau$  the imaginary time,  $\mathbf{q} = (k, \omega_n/u')$ ,  $\beta = 1/T$  and  $\Omega$  the length. In the limit

$\beta, \Omega \rightarrow \infty$ , the sum can be transformed into an integral and one obtains

$$G_\varphi(\mathbf{r}) = \frac{u'}{2\pi} \int_0^\Lambda q dq \int_0^{2\pi} d\theta_q \frac{1 - \cos(qr \cos(\theta_q))}{(u'q)^2 + (\Delta')^2}, \quad (\text{A8})$$

where  $\theta_q$  is the angle between  $\mathbf{q}$  and  $\mathbf{r}$ ,  $q = |\mathbf{q}|$  and  $r = |\mathbf{r}|$ . The result for  $G_\varphi(\mathbf{r})$  is

$$\begin{aligned} G_\varphi(r) &= \ln(\Lambda\xi) - K_0(r/\xi), \\ \xi &\equiv u'/\Delta', \\ r &\equiv \sqrt{x^2 + (u'\tau)^2} \end{aligned} \quad (\text{A9})$$

where  $K_0(z)$  is the modified Bessel function. Using the asymptotic and series expansions of  $K_0(z)$  for large and small arguments

$$K_0(z \gg 1) \approx \sqrt{\frac{\pi}{z}} e^{-z}, \quad K_0(z \ll 1) \approx -\ln(z), \quad (\text{A10})$$

we obtain a result for  $C_\varphi$  [Eq. (A6)] in the two limits:

$$C_\varphi(r \ll \xi) \cong (r\Lambda)^{-2K'}, \quad C_\varphi(r \gg \xi) \cong (\Lambda\xi)^{-2K'}. \quad (\text{A11})$$

Finally, employing Eq. (A3), this yields the correlation functions [Eq. (A4)] in the limit  $r \gg \xi$ :

$$\begin{aligned} \chi_{uu} &\cong \cos^2(\alpha) (\Lambda\xi)^{-2K'}, \quad \chi_{lt} \cong \frac{1}{2} \sin(2\alpha) (\Lambda\xi)^{-2K'}, \\ \chi_{tt} &\cong \sin^2(\alpha) (\Lambda\xi)^{-2K'}. \end{aligned} \quad (\text{A12})$$

- 
- <sup>1</sup> H. Bethe, Z. Phys. **71**, 205 (1931).  
<sup>2</sup> L. Balents, Nature **464**, 199 (2010).  
<sup>3</sup> E. Dagotto, J. Riera and D. Scalapino, Phys. Rev. B **45**, 5744 (1992).  
<sup>4</sup> T. M. Rice, S. Gopalan and M. Sigrist, Europhys. Lett. **23**, 445 (1993).  
<sup>5</sup> T. M. Rice, S. Gopalan and M. Sigrist, Physica B, **199**, 378 (1994).  
<sup>6</sup> H. J. Schulz, Phys. Rev. Lett. **77**, 2790 (1996).  
<sup>7</sup> F. H. L. Essler, A.M. Tsvelik, and G. Delfino, Phys. Rev. B **56**, 11001 (1997).  
<sup>8</sup> A. A. Nersesyan and A. M. Tsvelik, Phys. Rev. B **67** 024422 (2003).  
<sup>9</sup> P. W. Anderson, Mater. Res. Bull. **8**, 153 (1973).  
<sup>10</sup> S. Moukouri, Phys. Rev. B **70**, 014403 (2004).  
<sup>11</sup> O. A. Starykh and L. Balents, Phys Rev. Lett. **93** 127202 (2004).  
<sup>12</sup> T. Hikihara and O. A. Starykh, Phys. Rev. B **81** 064432 (2010).  
<sup>13</sup> P. Sindzingre, Phys. Rev. B **69**, 094418 (2004).  
<sup>14</sup> O. Volkova, I. Morozov, V. Shutov, E. Lapsheva, P. Sindzingre, O. Cépas, M. Yehia, V. Kataev, R. Klingeler, B. Büchner, and A. Vasiliev, Phys. Rev. B **82**, 054413 (2010).  
<sup>15</sup> V. Gnezdilov, P. Lemmens, Yu. G. Pashkevich, D. Wulferding, I. V. Morozov, O. S. Volkova, and A. Vasiliev, Phys Rev B **85** 214403 (2012)  
<sup>16</sup> E. Shimshoni, N. Andrei and A. Rosch, Phys. Rev. B **68** 104401 (2003).  
<sup>17</sup> O. Shlagman and E. Shimshoni, Phys. Rev. B **86** 075442 (2012)  
<sup>18</sup> F. D. M. Haldane, Phys. Lett., **93A**, 464, (1983); F. D. M. Haldane, Phys. Rev. Lett., **50**, 1153, (1983).  
<sup>19</sup> D. G. Shelton, A. A. Nersesyan, and A. M. Tsvelik, Phys. Rev. B **53** 8521 (1996)  
<sup>20</sup> A. O. Gogolin, A. A. Nersesyan, and A. M. Tsvelik, *Bosonization and Strongly Correlated System* (Cambridge University Press, Cambridge, England 1998)  
<sup>21</sup> T. Giamarchi, *Quantum Physics in One Dimension* (Oxford University Press, 2004).  
<sup>22</sup> P. Lecheminant, A. O. Gogolin, and A. Nersesyan, Nuclear Phys. B **639**, 502 (2002).  
<sup>23</sup> Note that in this limit, our derivation does not strictly apply since the underlying assumption of weak rung-coupling approximation breaks down.